International Conference on Mathematics, Computational Methods & Reactor Physics (M&C 2009)
Saratoga Springs, New York, May 3-7, 2009, on CD-ROM, American Nuclear Society, LaGrange Park, IL (2009)

MULTIDETECTOR CT (MDCT) MODELING FOR ORGAN DOSE ASSESSMENTS OF VARIOUS PATIENT PHANTOMS

Jianwei Gu, Peter F. Caracappa, X. George X*
Nuclear Engineering and Engineering Physics Program
Rensselaer Polytechnic Institute
Troy, NY 12180
*xug2@rpi.edu

ABSTRACT

Multiple-detector computed tomography (MDCT), a diagnostic imaging modality that is rapidly evolving, has caused an increased concern about the potential radiation risk to the patient. The need for assessing radiation dose associated with the associated MDCT protocols can be met by the use of Monte Carlo-based CT source models that are integrated with patient computational phantoms for organ dose calculations. This paper summarizes our work on the development and application of an MDCT scanner model using the Monte Carlo methods. The MCNPX code was used to simulate the x-ray source including the energy spectrum, filter, and scan trajectory. Detailed GE LightSpeed CT scanner components were specified using an iterative trial-and-error procedure. The scanner model was validated by comparing simulated results against measured CTDI values. The validated scanner model was then integrated with various phantoms, including RPI Adult Male phantom, RPI Adult Female phantom, RPI-P regnant Female phantoms in three different gestational periods to calculate organ doses. Organ doses are compared for different phantoms. Also, it was found that the dose to the fetus of the 3-, 6-and 9-month was 0.13 mGy/100mAs, 0.21mGy/100mAs, and 0.26mGy/100mAs, respectively. This work demonstrates the feasibility of modeling and validating MDCT scanner by Monte Carlo methods, as well as assessing organ dose by combining the MDCT scanner model and patient phantoms.

Key Words: Multi-detector computed tomography, Monte Carlo, organ dose, patient phantom

1. INTRODUCTION

Computed tomography (CT), as a preeminent diagnostic imaging modality, has been known to contribute a significant portion of the overall radiation dose received by patients from diagnostic procedures [1-12]. The advent of multi-detector CT (MDCT) has fueled a dramatic increase in use of CT, and the radiation exposures associated with various CT scan protocols have been studied extensively [4-11]. There is a consensus from the medical physics community that an increase in MDCT utilization must be accompanied by a heightened understanding of radiation dose and risk [12]. The American College of Radiology has issued a strong recommendation on tracking and reporting patient-specific exposures and resulting organ doses [13].

Compared with physical measurements, voxelized patient phantoms and modeled MDCT scanner based computational dosimetry provides a more convenient alternative to track and report CT doses. Using Monte Carlo methods, several research groups have simulated the CT sources and assessed doses to adult, pediatric and pregnant patients [14-17]. However, an

insufficient level of detail on the CT parameters was reported in these papers and it has been difficult for others to repeat or to compare results.

The current study in this paper was motivated by the absence of detailed steps of the MDCT scanner model development and validation. The same methodology can be used to facilitate the study of MDCT dosimetry involving anatomically-realistic computational patient phantoms. This paper describes the development, validation and application of a Monte Carlo model of a GE LightSpeed 16-MDCT scanner. For validation, CTDI values for several different kVp values, as well as dose profiles were used to compare and fine-tune the parameters in the MDCT scanner model. Using the validated MDCT scanner model in combination with a set of pregnant patient phantoms representing 3-, 6- and 9- month gestational periods [18] radiation doses to the mother and fetus were calculated for selected imaging procedures. The RPI Adult Male and Female phantoms were also included in the model of MDCT scanner for assessment of CT dose for adult patients.

2. MATERIALS AND METHODS

The general workflow of the MDCT modeling, validation and application procedure in this study is illustrated in Fig. 1. It starts with determining MDCT source parameters including the x-ray source energy spectrum, internal filter, external filter (bow-tie filter), beam shape, etc. These parts together can be regarded as the MDCT scanner model. Once these parts as well as the CTDI body phantom have been defined, the Monte Carlo simulations obtain the CTDI center dose values (CTDIc), CTDI peripheral dose values (CTDIp) and the dose profiles along the surface of the CTDI body phantom. Then the reference values from the literature or the physical measurements are used to compare with the simulated values in order to validate the modeled MDCT scanner and its movement. When the scanner is validated, the CTDI phantom is replaced by the patient phantom and the Monte Carlo simulations are performed to assess the doses to the patient.

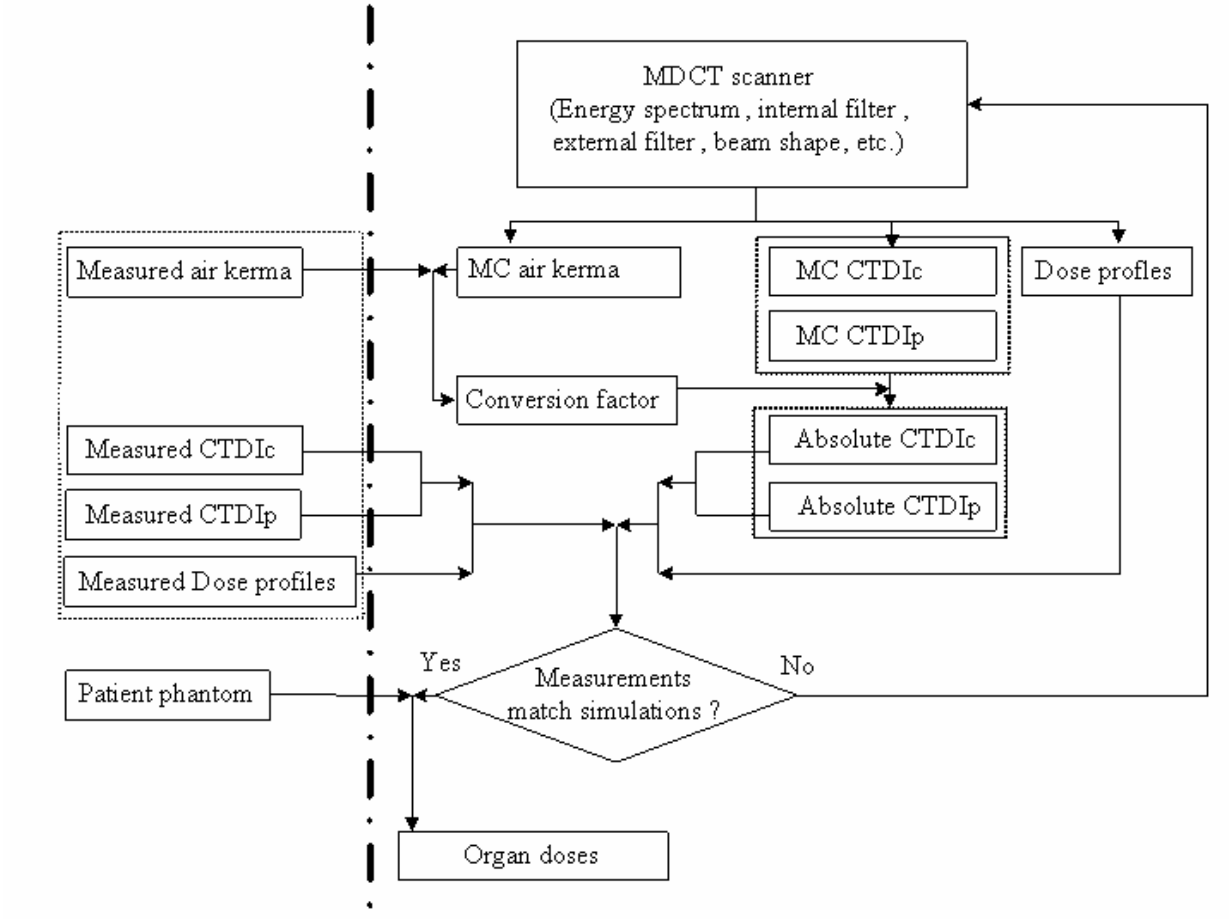

Figure 1. Flowchart for development, validation and application of the MDCT models.

In this flowchart, the left side of the vertical dash line indicates the work or data provided by the literature or previous research. All the measured data in this research were those reported by DeMarco *et al.* [16]. The patient phantoms were developed by Xu *et al.* [18]. The right side of the vertical dash line indicates the simulations and calculations in this study.

2.1. Monte Carlo Simulations

In this research, the MCNPX 2.5.0 code was used for all simulations, including CT scanner modeling, patient phantoms modeling, as well as dose computing [19]. MCNPX is a general purpose Monte Carlo radiation transport code that tracks all particles at all energies necessary for these simulations. The MCNPX package provides geometry modeling based on a combinatorial system using planes, cylinders, cones and spheres. In this study, the photon physics mode with the default energy cut-off was used. The photon transport model creates electrons but assumes that they travel in the direction of the primary photon and that the electron energy is deposited at the photon interaction site to satisfy the condition of charged particle equilibrium (CPE), which is a valid assumption in the energy range of diagnostic x-rays. Under the conditions of CPE, the collision kerma is equal to absorbed dose and is recorded using the type 6 (F6:p) tally of the

MCNPX. In all simulations, the number of histories was selected to achieve relative errors less than 5% in most organs (or detectors), and less than 10% for organs with the very small volumes or located a large distances from the primary beam.

2.2. CT Scanner Modeling

The 16-MDCT scanner modeled here (a LightSpeed 16, General Electric Healthcare Corporation, Waukesha, WI) is a third-generation MDCT, with 16 rows of 0.625mm wide detectors as well as eight rows of 1.25 mm detectors. It offers the user the following x-ray beam collimation options (given in the format of N × T, where N represents the number of data channels and T represents the nominal width of each data channel; each data channel may represent at least one detector row [5]: 16 × 0.625 mm (8 × 1.25 mm), 16 × 1.25 mm (8 × 2.5mm), as well as 2 × 0.625 mm and 1 × 5 mm modes. The scanner can operate in both axial and helical modes. For the helical scan, the pitch can be selected as 0.625, 0.875, 1.35 or 1.675 in the 8-channel mode or 0.5625, 0.9375, 1.375 or 1.75 in the 16-channel mode [16]. The system supports nominal x-ray energies of 80, 100, 120 and 140 kVp. X-ray beam shaping filtration including both head and body bowtie filters are equipped and used to compensate for the variation in body thickness across the transverse sections of the body, improving the image quality and reducing the dose to the peripheral region of the body. The distance from the focal spot to the isocenter (SID) is 54 cm, and the distance from the focal spot to the detector (SDD) is 95 cm. The fan beam is collimated in the x-y plane to a fan angle of 55^{o}.

2.3. Phantom Modeling

These RPI Adult Male (RPI-AM) and RPI Adult Female (RPI-AF) phantoms, as illustrated in Fig 2 (a) and (b), were constructed using surface mesh data for many anatomical features. The mesh-based organ models were created referencing the VIP-Man model and other anatomical images, and the organs were deformed to properly match ICRP recommendations. In a final step, the adjusted phantom is then converted into cubic voxels for use in Monte Carlo calculations [20]. The RPI-AM consists of 24650750 (153 × 125 × 653) cubic voxels with 0.27 cm on each side, and the RPI AF consists of 24466832 (247×151×656) cubic voxels with 0.25 cm on each side. In total, 28 different material compositions were defined and appropriately assigned to 122 separate organs or tissues for the Adult Male and 121 organs or tissues for the Adult Female. The reference values of elemental compositions of the organs and tissues as well as the mass densities were derived from ICRU Report 46 [21].

A set of realistic computational phantoms of a pregnant patient at the end of three gestational periods of 3, 6 and 9 months — called RPI-P3, RPI-P6 and RPI-P9 phantoms — were previously developed at RPI [18]. In RPI-P3, RPI-P6 and RPI-P9 phantoms, organ volumes and masses were carefully adjusted to agree with reference values recommended in the ICRP Publication 89 [22]. A total of 35 organs and tissues were included. The particular emphasis was placed on developing a realistic representation of fetus that consists of the skeleton (except for the 3-month phantom), brain, and soft tissue. Organs were voxelized with a resolution of 3 mm × 3 mm × 3 mm, and each phantom contains a total of about 25 million voxels. The RPI-P phantoms,

illustrated in Fig 2 (c)-(e), were finally implemented into MCNPX for dose calculations. The arms of the phantoms RPI-P3, -P6, -P9 and RPI-AM were removed in the simulations due to the clinical practice of lifting arms over head. However, the arms of the phantom RPI-AF remained due to the limitation of the phantom.

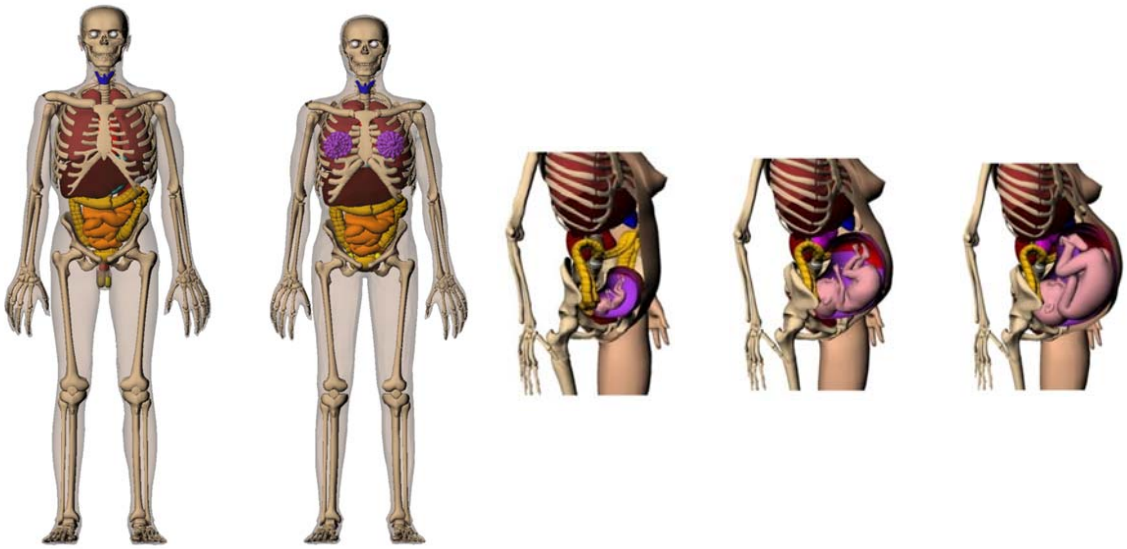

(a) RPI-AM (b) RPI-AF (c) RPI P3 (d) RPI P6 (e) RPI P9

Figure 2. Three-dimensional visualization of patient phantoms.

2.3. Organ Dose Calculations

The F6:p tally results in MCNPX are normalized per source history. In order to determine the absorbed dose from each CT scan procedure, the tally values in units of MeV/gram/source particle were converted to absorbed dose in units of mGy/100mAs by a conversion factor (CF). The CFs used in this study has been described previously [23], as a function of both beam energy *E* and beam collimation NT. In the current study, it is modified and defined as,

$$(CF)_{E,NT} = \frac{(CTDI_{100,\text{ air, measured per 100 mAs}})_{E,NT}}{(CTDI_{100,\text{ air, simulated per particle}})_{E,NT}}, \quad (1)$$

where $(CTDI_{100,\text{ air, measured per 100 mAs}})_{E,NT}$ in unit of mGy/100mAs is measured by the ion chamber in air at the scanner isocenter (see Appendix A), and $(CTDI_{100,\text{ air, simulated per particle}})_{E,NT}$ in unit of MeV/gram/particle is obtained by simulating the ion chamber under the same scan protocol. The absorbed dose to the organ or tissue in unit of mGy/100mAs is,

$$D_{\text{absolute}} = D_{\text{simulated}} \times CF \times N, \quad (2)$$

and *N* is the number of x-ray tube rotation during this CT scan. If the clinical tube current (mA) a nd exposure time (s) per rotation are known, the final absorbed dose in unit of mGy is,

$$D_{\text{total}} = D_{\text{absolute}} \times K \tag{3}$$

and here K is the ratio of mAs per rotation to 100 mAs. In this study, we reported the organ dose in unit of mGy/100mAs based on Eq. 2.

In order to validate the MDCT scanner model developed in this research, the body CTDI phantom was modeled and CTDI values were calculated and compared with the measured values. The CTDI values were determined by taking the product of the normalized CTDI dose calculated by MCNPX and the kVp-dependent conversion factor. The kVp-dependent conversion factors were calculated from single axial scans simulated free-in-air at the scanner isocenter for tube potentials of 80, 100, 120 and 140 kVp using the 20 mm beam collimation with the body bowtie filter.

3. RESULTS AND DISCUSSION

3.1. Validation of MDCT Scanner Modeling

The conversion factors for each kVp value are listed in Table I. for converting the Monte Carlo simulation results from MeV/gram per source particle to mGy/100mAs for the LightSpeed MDCT scanner. The percent relative error for the MCNPX results is less than 5%. The measurements [16] and MCNPX simulations were performed in air using the body bowtie filter. Using these conversion factors, the simulated CTDI values (air-kerma values at the center and at the 12:00 peripheral position of the CTDI phantom) were calculated and are shown in Table II, showing comparison of measured and simulated dose results from a single axial scan in the CTDI body phantom using the LightSpeed scanner operated at 120 kVp and 100 mAs. All scans used a 20-mm beam collimation and a body bowtie filter. The duration of the scan was 1 second. The Monte Carlo simulated CTDI values at the center showed good agreement with measured values.

Table I. Conversion factors for converting the Monte Carlo simulation results

kVp	Beam collimation (mm)	Measured $CTDI_{100}$ in air (mGy/100mAs)	Simulated $CTDI_{100}$ in air (MeV/gram/particle)	Conversion factor (mGy·gram·particle /100mAs/MeV)
80	4x5	8.10	7.15E-06	1.13E+06
100	4x5	14.70	8.34E-06	1.76E+06
120	4x5	22.71	9.33E-06	2.44E+06
140	4x5	31.93	1.03E-05	3.11E+06

Table II. Comparison of measured and simulated dose results

kVp	Position	Measured dose (mGy/100mAs)	Monte Carlo simulation (mGy/100mAs)	% Difference
80	Center	1.34	1.30	-2.80
	Peripheral	3.45	3.43	-0.60
100	Center	2.97	2.86	-3.77
	Peripheral	6.66	6.79	1.89
120	Center	5.12	4.98	-2.78
	Peripheral	10.48	10.97	4.69
140	Center	7.65	7.52	-1.76
	Peripheral	15.01	15.87	5.72

3.2. Organ Doses

Following the validation of the MDCT source modeling, this section describes the calculated doses to the RPI-AM, -AF and pregnant mother and fetus from maternal body chest CT scans. In all the simulations involving the patient phantoms, 10 million initial photons were sampled to guarantee statistical uncertainties less than 5% for the absorbed doses to the organs in the field of view (FOV).

As described previously, the organ doses to the patient phantoms (RPI-AM, -AF, RPI-P3, -6, and -9) from helical scans were assessed for a tube potential of 120 kVp and a pitch of 1.375. All MCNPX dose values were converted to absorbed dose in unit of mGy/100mAs by the corresponding CFs shown in Table I.

From the calculated results, the common organs among these five phantoms were selected, and the doses were reported accordingly. Fig. 3 indicates that the similar doses were delivered to the organs with same name in different phantoms. This phenomenon shows that the doses to the specific phantom can be studied through study on other similar phantoms. For example, the organ doses of pregnant patients could be assessed by studying the adult patient phantoms.

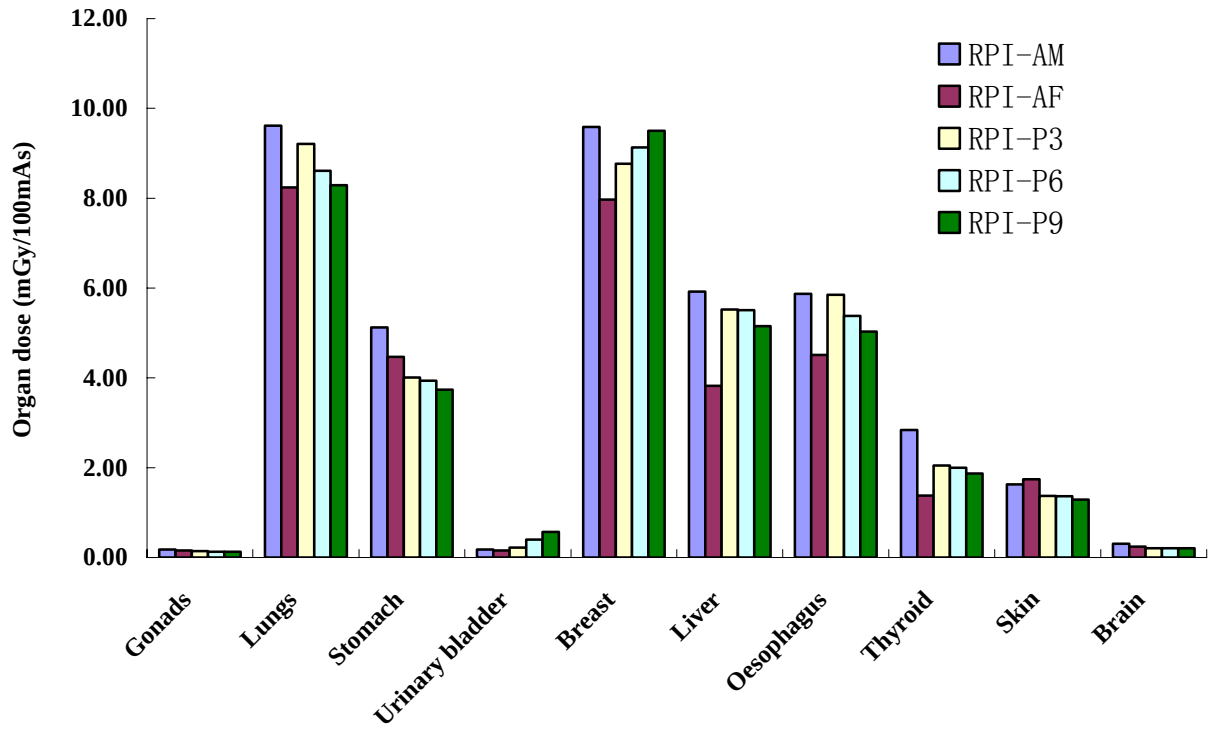

Figure 3. Doses to selected organs of the phantoms RPI-AM, RPI-AF and RPI-P3, -P6, -P9

The dose to the fetal total is the mass weighted average of the doses to the fetal soft tissue, fetal skeleton and fetal brain. The fetal total dose for the chest scan of the RPI-P3, P6 and P9 phantoms were 0.13 mGy/100mAs, 0.21 mGy/100mAs and 0.26 mGy/100mAs, respectively, as illustrated in Fig. 4. Assessment of the risk associated with radiation exposure of the fetus during MDCT scans of pregnant patients is of an increasing interest [1]. Based on the results by Hurwitz *et al.*[24], ICRP Publication 102 presents a summary of results from a phantom study using the protocols for imaging pregnant patients with suspected pulmonary embolism, appendicitis, and renal stones [1]. In a different publication, ICRP Publication 103 suggests that absorbed doses below 100 mGy to the embryo/fetus should not be considered a reason for terminating a pregnancy [25]. At embryo/fetus doses above this level, the pregnant patient should receive sufficient information to be able to make informed decisions based upon individual circumstances, including the magnitude of the estimated embryonic/fetal dose and the consequent risks of serious harm to the developing embryo/fetus and risks of cancer in later life [25]. Furthermore, the AAPM Task Group 36 (TG-36) provided a general summary of the risk to the fetus as a function of radiation dose for radiotherapy [26]. According to TG-36, the risk of normal tissue damage from fetal doses less than 50 mGy are negligible. Assuming a total of 300 mAs is applied to each scan, one obtains a fetal dose far below 50 mGy, and therefore the risk is negligible for a fetus of the RPI pregnant patient phantom when MDCT chest scan is performed.

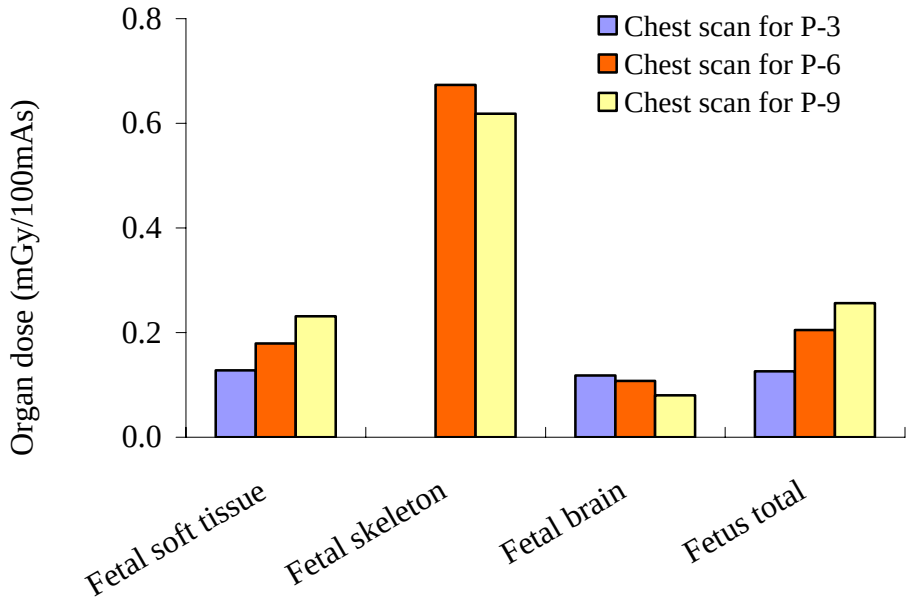

Figure 4. Comparison of doses to the 3-, 6-, and 9-month fetuses from chest scans of pregnant patients.

4. CONCLUSIONS

Since MDCT is increasingly popular, the need to assess and manage the potential exposures and associated radiation risk can be met by using Monte Carlo models of these modalities as well as anatomical realistic patient computational phantoms. This paper described the development and validation of Monte Carlo models of an MDCT scanner, and the application of these models for calculation of absorbed doses to the mother and fetus, as well as the adult patients, using selected MDCT scanning protocols. Detailed MDCT models including energy spectrum, filters, source geometry and movement under different scan modes were developed. The models were validated by comparing calculated center and peripheral CTDI dose values and dose profile curves to measurement data that reported in the literature. The validated x-ray source model and the helical source movement model were then integrated with the patient phantoms for assessments of organ doses or effective doses. The results on organ doses from specific CT procedures demonstrate the usefulness of the Monte Carlo based MDCT and patient models.

ACKNOWLEDGMENTS

This study was partially supported by a grant from the National Cancer Institute (R01CA116743).

REFERENCES

1. International Commission on Radiological Protection, “Managing Patient Dose in Multi-Detector Computed Tomography (MDCT),” ICRP Publication 102, Ann ICRP **37** (1) (2007).

2. F.A. Mettler, “Magnitude of radiation uses and doses in the United States: NCRP Scientific Committee 6-2 analysis of medical exposures,” Presented at: Advances in Radiation Protection in Medicine (2007).
3. P. C. Shrimpton and S. Edyvean, “CT scanner dosimetry,” Br. J. Radiol **71**, 1–3 (1998).
4. D. J. Brenner and E. J. Hall, D. Phil, “Computed Tomography — An Increasing Source of Radiation Exposure,” NEJM **357**, 2277-2284(2007).
5. What's NEXT? Nationwide Evaluation of X-ray Trends: 2000 computed tomography. (CRCPD publication no. NEXT_2000CT-T.) Conference of Radiation Control Program Directors, Department of Health and Human Services, 2006. (Accessed November 5, 2007, at http://www.crcpd.org/Pubs/NextTrifolds/NEXT2000CT_T.pdf).
6. D. J. Brenner, M. A. Georgsson, “Mass screening with CT colonography: should the radiation exposure be of concern?” Gastroenterology **129**, 328-337 (2005).
7. D. J. Brenner, “Radiation risks potentially associated with low-dose CT screening of adult smokers for lung cancer,” Radiology **231**, 440-445 (2004).
8. D. J. Brenner, C. D. Elliston, “Estimated radiation risks potentially associated with full-body CT screening,” Radiology **232**, 735-738 (2004).
9. D. J. Brenner, C. Elliston, E. Hall, W. Berdon, “Estimated risks of radiationinduced fatal cancer from pediatric CT,” AJR Am J Roentgenol **176**, 289–296 (2001).
10. W. Huda, A. Vance, “Patient doses in adult and pediatric CT,” AJR Am J Roentgenol **188**, 540–546 (2007).
11. M. F. McNitt-Gray, “Radiation issues in computed tomography screening,” Semin Roentgenol **38**, 87–99 (2003).
12. The Measurement, Reporting, and Management of Radiation Dose in CT, Report of AAPM Task Group 23 of the Diagnostic Imaging Council CT Committee, 2008 (accessed at: http://www.aapm.org/pubs/reports/rpt_96.pdf)
13. E. S. Amis, P. F. Butler, K. E. Applegate, *et al*, “American College of Radiology white paper on radiation dose in medicine,” J Am Coll Radiol. **4**, 272-284 (2007).
14. Peter F. Caracappa, “Investigation of patient dose from CT examination using the VIP-Man model,” thesis for master of science, 2001 (unpublished).
15. H. T. Winer-Muram, J. M. Boone, H. L. Brown, S. G. Jennings, W. C. Mabie, G. T. Lombardo, “Pulmonary embolism in pregnant patients: fetal radiation dose with helical CT,” Radiology **224**, 487– 492 (2002).
16. J. J. DeMarco, C. H. Cagnon, D. D. Cody, D. M. Stevens, C. H. McCollough, J. O'Daniel, and M. F. McNitt-Gray, “A Monte Carlo based method to estimate radiation dose from multidetector CT (MDCT): cylindrical and anthropomorphic phantoms,” Phys. Med. Biol. **50**, 3989-4004 (2005).
17. P. Deak, “Validation of a Monte Carlo tool for patient-specific dose simulations in multi-slice computed tomography,” Eur Radiol **18**, 759–772 (2008).
18. X. G. Xu, V. Taranenko, J. Zhang, and C. Shi, “A boundary-representation method for designing whole-body radiation dosimetry models: pregnant females at the ends of three gestational periods—RPI-P3, -P6 and -P9,” Phys. Med. Biol. **52**, 7023– 044 (2007).
19. D. B. Pelowitz, “MCNPX^{TM} USER’S MANUAL Version 2.5.0,” (2005)
20. J. Zhang, Y. Na, and X. G. Xu, “Development of a pair of mesh-based adult male and female computational phantoms and calculations of organ doses for monoenergetic photon beams,” Physics in Medicine and Biology. (In press)

21. International Commission on Radiation Units and Measurements, “Photon, electron, proton and neutron interaction data for body tissues,” ICRU Report 46, Bethesda, Md., USA (1992).
22. International Commission on Radiological Protection, “Basic Anatomical and Physiological Data for Use in Radiological Protection: Reference Values,” ICRP Publication 89, Ann ICRP **32**(3-4), 1-277 (2003).
23. G. Jarry, J. J. DeMarco, and M. F. McNitt-Gray, “Monte Carlo dose verification of a commercial CT scanner with applications for patient specific dosimetry,” Med. Phys. **29**, 1344 (2002)..
24. L. M. Hurwitz, T. Yoshizumi, R. E. Reiman, C. G. Philip, K. P. Erik, P. F. Donald, T. Greta, N. Giao and B. Lottie, “Radiation Dose to the Fetus from Body MDCT During Early Gestation,” Am. J. Roentgenol. **186**, 871-6 (2006).
25. International Commission on Radiological Protection, “Recommendations of the ICRP,” ICRP Publication 103, Ann ICRP **37**, 1-332 (2007).
26. M. Stovall, C. R. Blackwell, J. Cundiff, D. H. Novack, J. R. Palta, L. K. Wagner, E. W. Webster and R. J. Shalek, “Fetal dose from radiotherapy with photon beams: Report of AAPM Radiation Therapy Committee Task Group No. 36,” Med. Phys. **22**, 63-82 (1995).

APPENDIX A

Here we define the nominal beam width is T, the area of the cross-section of the ion-chamber with length L and mass M. So the $CTDI_{100}$ is defined as,

$$\begin{aligned}
CTDI_{100} &= \frac{1}{T}\int_{-50}^{50} D(z)\bullet dz \\
&= \frac{1}{T}\int_{-50}^{50} \frac{de}{dm}\bullet dz \\
&= \frac{1}{T}\int_{-50}^{50} \frac{de}{\rho\bullet S\bullet dz}\bullet dz \\
&= \frac{1}{T}\int_{-50}^{50} \frac{de}{\rho\bullet S} \\
&= \frac{1}{T}\bullet\frac{1}{\rho\bullet S}\bullet\int_{-50}^{50} de \\
&= \frac{1}{T}\bullet\frac{1}{\frac{M}{L}}\bullet\int_{-50}^{50} de \\
&= \frac{L}{T}\bullet\frac{\int_{-50}^{50} de}{M} \\
&= \frac{L}{T}\bullet D_{average}
\end{aligned}$$

Here the Daverage is the measured dose from the ion-chamber or the simulated dose to the active volume of the modeled ion-chamber from Monte Carlo simulation.